PHYSICAL REVIEW B VOLUME 22, NUMBER 10 15 NOVEMBER 1980

Stress dependence of the nitrogen-bound excitons in GaP:N

H. Mathieu, L. Bayo,* J. Camassel, and P. Merle
Centre d'Etudes d'Electronique des Solides,† Université des Sciences et Techniques du Languedoc, 34060-Montpellier Cedex, France
(Received 25 February 1980)

We investigate the effect of uniaxial compressions on the zero-phonon luminescence and absorption spectra of the nitrogen-bound excitons in GaP. All data have been collected at pumped-liquid-helium temperature for the stress directions [111], [110], and [001], respectively. The low-stress behavior of the exciton states is consistent with the simple j-j coupling scheme for the excitons, and the stress-induced splitting of the bound hole is found isotropic. The high-stress behavior is quantitatively consistent with an exciton wave function primarily associated with the $\langle 100\rangle$ conduction-band minima. The corresponding valley-orbit splitting is $E_{12}=24$ meV. Under stress, the valley-orbit coupling matrix element appears to be stress dependent. We find $\Delta = (8 + 4\times 10^{-4}X)$ meV. This result clearly shows that the nitrogen potential is also stress dependent. On the other hand, since the stress dependence of the exciton binding energy E_b cannot be accounted for by a combined X-L nature of the bound-electron wave function, it results from the stress dependence of the potential extension via the stress dependence of the valley-orbit coupling matrix element.

I. INTRODUCTION

Excitons bound to nitrogen in GaP (Refs. 1–5) and $GaAs_{1-x}P_x$,[6–13] have been studied extensively for several reasons. One reason is their radiative efficiency, making GaP:N and $GaAs_{1-x}P_x$:N useful in light-emitting devices. A more fundamental reason is the basic problem of the process by which an exciton binds to an isoelectronic trap. The state of the art has been clearly described in a very recent review on bound excitons in semiconductors by Dean and Herbert.[14]

Several theoretical attempts have been made to explain the binding of excitons to nitrogen, both in GaP (Refs. 15–17) and in $GaAs_{1-x}P_x$.[6,11,12] A review of the different models is given by Hsu *et al.*[12] The main conclusion which can be drawn is that the one-band one-site Koster-Slater model is not adequate to describe all aspects of the problem. In particular, this model fails to explain in $GaAs_{1-x}P_x$ (i) the existence of two bound energy levels per trap N_Γ and N_X and (ii) the alloy composition dependence of the binding energy of the exciton (even taking into account the different composition dependence of Γ, X, and L minima). It is then clear that the lattice relaxation around the smaller N atom and the electronic-charge redistribution must be included in the effective potential and, in order to explain the composition dependence of the exciton binding energy, the zero-range composition-independent Koster-Slater potential had to be replaced by a spatially extended composition-dependent potential.[12]

To obtain knowledge of the binding mechanism of excitons to isolated nitrogen in GaP and $GaAs_{1-x}P_x$, the composition-dependence measurements of the low-temperature luminescence in $GaAs_{1-x}P_x$:N alloys have been very fruitful.[6–13] In this way a better insight into the binding mechanism might be attained through a detailed knowledge of the uniaxial-stress dependence of the bound-exciton states. This is the subject of the present report.

In both the one-band one-site approximation and the more elaborate computer calculation using a very-short-range potential,[15] the excited states due to intervalley mixing were found to be unbound. This results from the very-short-range nature of the potential which gives rise to a very important intervalley splitting $E_{12}=E(\Gamma_{12})-E(\Gamma_1)$. Using a Gaussian potential with adjustable range (A), Faulkner[15] has reported that E_{12}, which is a fairly sensitive function of the range, is essentially zero at $A=8$ Å and greater than 10 meV at $A\simeq 5$ Å. The knowledge of this splitting is then of great importance for estimation of the potential range. But it is rather difficult to get E_{12} directly from experimental optical spectra for several reasons. First, in visible spectroscopy (creation or recombination of bound excitons) the only state which is radiative is the Γ_1 ground state because of its strong admixture with the direct minimum of the conduction band. In contrast, the antisymmetric Γ_{12} state, which is not admixed, has zero no-phonon oscillator strength. Second, in infrared spectroscopy the transition $\Gamma_1 \rightarrow \Gamma_{12}$ is dipole forbidden. Third, electronic Raman scattering, which has been used to obtain E_{12} for a donor in GaP:S, Se, Te,[18] may not be used because the Γ_1 ground state is empty without optical excitation. And fourth, if the Γ_{12} state is unbound as suggested by Faulkner's calculations, it must be observed above the threshold of the excitonic band gap, which is very difficult. As a consequence, no report of E_{12} has been given. Previous misguided speculation about the origin of GaP:N luminescence lines prompted the suggestion that

they were higher valley-orbit states giving $E_{12} \simeq 1$ meV.[15] However, a detailed investigation[1] of the behavior of these lines has shown that they result from the radiative recombination of one of the two excitons comprising a bound excitonic molecule.

Under calibrated uniaxial stress it is possible to determine E_{12} unambiguously. Remember that a shear strain destroys the equivalence of the three conduction-band valleys at X and modifies the nitrogen state by the so-called "valley-repopulation effect."[19] This has the effect of admixing the doublet state Γ_{12} into the singlet ground state Γ_1. The result is a nonlinear stress-induced shift of the ground state. We have obtained $E_{12} = 24$ meV.

On the other hand, just as the different composition dependences of the X, Γ, and L conduction-band minima cannot explain the observed composition dependence of exciton binding energy in $GaAs_{1-x}P_x$:N, we show that the different stress dependence of X, Γ, and L cannot explain the observed stress dependence of the binding energy in GaP:N. This stress dependence must be associated with a stress dependence of the nitrogen potential. The stress-induced increase of the potential range results in a weakening of the intervalley mixing.

Two interesting papers have already been published on the uniaxial-stress behavior of the N exciton in GaP. Merz *et al.*[20] have made a comparative study of the stress dependence of the binding energy of the S, Bi, and N excitons in GaP, but in all cases the stress was applied along the [111] direction only. Pollak *et al.*[21] have investigated the effect of uniaxial compression along [111], [001], and [110] directions on the modulated-transmission spectra of N exciton and N-N pairs, but they presented the experimental results without going into details of the analysis.

II. EXPERIMENTAL

The GaP single crystals used in this experiment were obtained from Dr. Poiblaud, Radiotechnique, Compelec (Caen, France). Suitably pure starting GaP polycrystalline material was presynthesized by a gallium-solution growth process, giving a residual doping concentration as low as 10^{15} cm^{-3}. Nitrogen-doped crystals pulled from this material have N concentration in the range 10^{16}–10^{17} cm^{-3}. All samples were x-ray oriented and cut along a [111], [001], or [110] direction. This resulted in small parallelepipedic samples of approximate dimensions $1\times1\times10$ mm^3. The A and B absorption and luminescence lines were investigated at pumped-liquid-helium temperature using a conventional stressing apparatus already described.[19]

III. THEORETICAL BACKGROUND

A. Zero-stress bound-exciton state

A very good review of impurity states in semiconductors has been given in a recent article by Bassani *et al.*[22] The problem is to solve the Schrödinger equation

$$(H_0 + U)|\phi\rangle = E|\phi\rangle , \tag{1}$$

where U is the impurity potential.

A natural choice of a complete basis for expanding the states is the set of Bloch states $|k\rangle$:

$$|\phi\rangle = \int dk\, \phi(k)|k\rangle . \tag{2}$$

Substituting Eq. (2) into Eq. (1), premultiplying by $\langle k|$, integrating over Ω, and making use of the orthogonality of the Bloch functions, one obtains the classical equation

$$[E(k) - E]\,\phi(k) + \int dk' U(kk')\phi(k') = 0 , \tag{3}$$

where $U(k,k') = \langle k|U|k'\rangle$. In order to solve Eq. (3), it is useful to divide the $\vec{k}$ space into subzones, each subzone being centered around a critical point. The integral equation (3) then splits into a system of coupled integral equations:

$$[E(k) - E]\phi_i(k) + \sum_j \int_{\Omega_j} dk' U_{ij}(kk')\phi_j(k') = 0 . \tag{4}$$

Now the respective contributions of each subzone depend (i) on the detail of the band structure and (ii) on the strength and real-space extension of the impurity potential. For a long-range, slowly varying potential, such as a Coulomb potential, most of the contribution comes from the Bloch functions near the band extrema. For a short-range potential, a large proportion of the wave function of the electron is located in the vicinity of the central cell. Since r and $\vec{k}$ are conjugate quantities, the wave function is much more extensive in $\vec{k}$ space and the appropriate set of basis functions is the set of Wannier functions $|R\rangle$. The Wannier functions are then generated from the Bloch functions by the classical formula and the matrix to be considered becomes finite because the matrix elements $\langle R|U|R'\rangle$ become negligible for sufficiently large R or R'. This calculation has been carried out for N in GaP by Faulkner,[15] using U of shorter range than the interatomic spacing.

Now several experiments performed in $GaAs_{1-x}P_x$ (Refs. 11 and 12) have shown that the lattice distortion around the N impurity plays a

significant role in binding an electron, so that the zero-ranged Koster-Slater potential must be replaced by a moderately extended potential. Moreover, low-temperature excitation[5] and absorption spectra (see Fig. 1) obtained from nitrogen-doped crystals of GaP present sharp structures corresponding to the ⟨100⟩ phonon replica of the principal A line. The presence and the sharpness of these structures indicate that almost all of the exciton wave function must be confined in $\vec{k}$ space to a limited volume around the X point. Confirmation of this hypothesis will be given by the uniaxial-stress dependences of the low-temperature absorption line (see discussion in Sec. VI). Consequently the sum over j in Eq. (4) may be reasonably limited to the three zones centered at the X points. On the other hand, since $U_{ij}(k,k')$ which connect different valleys is much smaller than $U_{ii}(k,k')$ in the same valley, Eq. (4) can be decoupled in the lowest order to obtain a set of three independent homogeneous equations:

$$[E(k)-E]\psi_i^0(k)+\int_{\Omega_i} dk' U_{ii}(k,k')\psi_i^0(k)=0, \quad i=1\text{–}3. \tag{5}$$

The wave function of the component associated with the valley X_i located at k_i is given by

$$\psi_i^0(k)=\int_k dk'\, a_0(k'-k_i)\,|k'\rangle. \tag{6}$$

Now the effect of $U_{ij}(k,k')$ terms which connect different valleys is calculated by expanding $\phi(k)$ in terms of the zero-order solutions $\psi_i^0(k)$ and substituting it into the original Eq. (4). We obtain the set of homogeneous equations:

$$(E_i^0-E)\alpha_i-\sum_{j\neq i}\alpha_j\Delta_{ij}=0, \tag{7}$$

where

$$\Delta_{ij}=-\int_{\Omega_i}\int_{\Omega_j} dk\,dk'\,\psi_i^{0*}(k)U_{ij}(k,k')\psi_j^0(k). \tag{8}$$

The three valleys being equivalent, all the E_i^0 values and all the Δ_{ij} values are the same and the eigenvalues of Eq. (4) are found as solutions of the determinant equation:

$$\det|(E^0-E)\delta_{ij}-(1-\delta_{ij})\Delta|=0. \tag{9}$$

The zero-order solution is a triplet state of energy E^0 and wave functions:

$$|\phi_i^0\rangle=\int_{\Omega_i} dk\,\psi_i^0(k)\,|k\rangle, \quad i=1\text{–}3. \tag{10}$$

In tetrahedral symmetry (T_d) the intervalley mixing splits this triplet into a singlet $\Gamma_1(\Gamma_6)$ of energy $E^0-2\Delta$ and a doublet $\Gamma_{12}(\Gamma_8)$ of energy $E^0+\Delta$. The wave functions are then

$$|\phi\rangle=\sum_i \alpha_i\,|\phi_i^0\rangle, \quad i=1\text{–}3, \tag{11}$$

where

$$\alpha_i=\begin{cases}\frac{1}{\sqrt{3}}(1,1,1) & (\Gamma_1 \text{ state}),\\ \frac{1}{\sqrt{6}}(-1,-1,2) & \\ \frac{1}{\sqrt{2}}(1,-1,0) & (\Gamma_{12} \text{ states}).\end{cases}$$

Now the bound-exciton state corresponds to the electron bound by the short-range nitrogen potential and the hole bound by the long-range Coulomb attraction of the electron. The ground state is made of an electron localized in the Γ_6 nitrogen state and a hole associated with the Γ_8 valence-band maximum. To zero order, the wave function which corresponds is a product of the electron wave function by the hole wave function times an envelope function. The resulting zero-order exciton states next couple by j-j interaction to form a $J=1$ triplet of energy $E=E_0+\frac{5}{8}\gamma$ and, at lower energy, a $J=2$ quintet of energy $E=E_0-\frac{3}{8}\gamma$. The transition between these states and the $J=0$ crystal ground state lead to A line (dipole allowed) and B line (dipole forbidden). The energy difference between A and B has been measured to be $\gamma=0.91$ meV. The effect of the crystal field is a mixing of the exciton basis states and hence a splitting of the $J=2$ state into a Γ_{12} doublet and a Γ_{15} triplet. This splitting, which is expected to be very small, has not been observed.

B. Stress dependence

The stress dependence of the bound-exciton states in an indirect semiconductor are discussed in detail for (D^0X) complexes in GaP:S,[19,23] for excitons bound to isoelectronic donors in GaP:Bi (Ref. 24), and for excitons bound to donor-acceptor pairs in GaP:Cd-O.[25] The stress dependence of the N excitons in GaP is analogous to the one reported for Bi excitons. However, in GaP, N is an isoelectronic acceptor while Bi is an isoelectronic donor. In other words, the mechanism for binding an exciton is different: The first one is attractive for the electron while the second is attractive for the hole. The result is that the stress-induced splittings of the bound-exciton states, which correspond to the splitting of the hole states, are expected to be different. These splittings have been observed to be very anisotropic for the Bi exciton[24] and isotropic for the N exciton (see Fig. 8). Consequently the stress dependence of the N exciton reduces to the isotropic-coupling case given for the Bi exciton by

Onton and Morgan.[24]

The strain field produced in a cubic crystal by a uniaxial stress can be split into the sum of hydrostatic part plus a shear part which depends on the stress direction.

1. Hydrostatic effect

The hydrostatic component induces only a shift of the center of gravity of the exciton, given by

$$A_h = a(S_{11}+2S_{12})X, \tag{12}$$

where a is the hydrostatic deformation potential of the bound exciton and S_{ij} are the elastic compliance constants of the crystal.

2. Shear effect

The shear component splits the valence band and lifts the degeneracy of the conduction-band valleys.

a. Valence-band-splitting effect

Taking account of the stress-induced coupling between Γ_{8v} and the spin-orbit split-off valence band, the splitting of the Γ_8 states into the V_1 ($|M|=\frac{1}{2}$) and V_2 ($|M|=\frac{3}{2}$) sublevels is given by[19]

$$V_1 = \epsilon + 2\epsilon'^2/(\Delta_0+\epsilon), \tag{13a}$$

$$V_2 = -\epsilon, \tag{13b}$$

where Δ_0 is the spin-orbit splitting of the valence band. ϵ and ϵ' are listed in Table I for the three principal stress directions.

The splitting of the valence band separates the $J=1$ and $J=2$ exciton states into series of sublevels (one for each value of $|M|$ quantized along the stress axis) and mixes those having the same value of M. Now, for the N exciton, on account of the relative magnitudes of the j-j interaction ($\gamma = 0.9$ meV) and of the valence-band splitting [$2\epsilon \simeq 4$ meV/kbar (Ref. 26)], the nonlinear behavior resulting from the stress-induced mixing of the $|JM\rangle$ states will be found only under very low stress conditions. In this case the nonlinear component of the V_1 stress-split valence band [Eq. (13a)] can be ignored and the shifts of the sublevels of the $J=1$ and $J=2$ states are given by[24]

$$E(|1,\pm1\rangle) = \gamma/8 + (\gamma^2/4 + \gamma\epsilon/2 + \epsilon^2)^{1/2}, \tag{14a}$$

$$E(|1,0\rangle) = \tfrac{5}{8}\gamma - \epsilon, \tag{14b}$$

$$E(|2,\pm2\rangle) = -\tfrac{3}{8}\gamma + \epsilon, \tag{14c}$$

$$E(|2,\pm1\rangle) = \tfrac{1}{8}\gamma - (\gamma^2/4 + \gamma\epsilon/2 + \epsilon^2)^{1/2}, \tag{14d}$$

$$E(|2,0\rangle) = -\tfrac{3}{8}\gamma - \epsilon. \tag{14e}$$

Please note that the symbol γ in Eqs. (14) corresponds to Δ in Eqs. (7) of Ref. 24. In the present work, Δ is restricted to represent the valley-orbit splitting matrix element as was done in Ref. 19.

In the high-stress range $\epsilon \gg \gamma$, Eqs. (14) can be simplified but we must take into account the nonlinear component of V_1 [Eq. (13a)]. The stress dependence of the sublevels are then given by

$$E(|1,\pm1\rangle) = \tfrac{3}{8}\gamma + \epsilon, \tag{15a}$$

$$E(|1,0\rangle) = \tfrac{5}{8}\gamma - \epsilon - 2\epsilon'^2/(\Delta_0+\epsilon), \tag{15b}$$

$$E(|2,\pm2\rangle) = -\tfrac{3}{8}\gamma + \epsilon, \tag{15c}$$

$$E(|2,\pm1\rangle) = -\tfrac{1}{8}\gamma - \epsilon - 2\epsilon'^2/(\Delta_0+\epsilon), \tag{15d}$$

$$E(|2,0\rangle) = -\tfrac{3}{8}\gamma - \epsilon - 2\epsilon'^2/(\Delta_0+\epsilon). \tag{15e}$$

b. Valley-repopulation effect

The shear strain lifts the degeneracy of the three conduction-band valleys and modifies the exciton states by the so-called valley-repopulation effect. This shifts and mixes between them the Γ_1 and Γ_{12} valley-orbit split states, giving rise to a nonlinear stress-induced shift of the ground state of the bound exciton. The treatment, based on the valley-repopulation model, has been developed by Price[27] for donors in germanium and successfully used by Wilson and Feher[28] for donors in silicon, by Onton and Morgan[24] for Bi excitons in GaP:Bi, and by Mathieu *et al.*[19] for (D^0X) complexes in GaP:S. The shear-strain dependence of the electron states of the exciton are given by[19]

TABLE I. Stress dependence of the parameters ϵ, ϵ', and S with applied uniaxial stress along [111], [001], or [110]. The results are listed according to the notation of Ref. 19. b_1 and d_1 are pure orbital deformation potentials for a strain of tetragonal and trigonal symmetry, respectively. b_2 and d_2 are spin-dependent deformation potentials. S_{ij} are the elastic compliance constants.

Stress direction	ϵ	ϵ'	S
[111]	$\frac{d_1+2d_2}{2\sqrt{3}} S_{44}X$	$\frac{d_1-d_2}{2\sqrt{3}} S_{44}X$	0
[001]	$(b_1+2b_2)(S_{11}-S_{12})X$	$(b_1-b_2)(S_{11}-S_{12})X$	$2(S_{11}-S_{12})X$
[110]	$\frac{1}{4}(\epsilon_{001}+3\epsilon_{111})$	$\frac{1}{4}(\epsilon'_{001}+3\epsilon'_{111})$	$-(S_{11}-S_{12})X$

$$E(\Gamma_1) = \tfrac{1}{2}\Delta[-1 + x - 3(1 + \tfrac{2}{3}x + x^2)^{1/2}] , \quad (16a)$$

$$E(\Gamma_{12}^a) = \tfrac{1}{2}\Delta[-1 + x + 3(1 + \tfrac{2}{3}x + x^2)^{1/2}] , \quad (16b)$$

$$E(\Gamma_{12}^b) = \Delta(1 - x) , \quad (16c)$$

with

$$x = E_2 S/6\Delta .$$

Δ is the intervalley-coupling matrix element [Eq. (8)], and E_2 is the shear deformation potential of the conduction band. S is given in Table I for the different stress directions.

The resulting stress dependence and selection rules of the bound-exciton ground state is then given by

$$A^+ = E_0 + A_h + E(\Gamma_1) + E(|1, \pm 1\rangle) \quad (\sigma) , \quad (17a)$$

$$A^- = E_0 + A_h + E(\Gamma_1) + E(|1, 0\rangle) \quad (\sigma, \pi) , \quad (17b)$$

$$B^+ = E_0 + A_h + E(\Gamma_1) + E(|2, \pm 2\rangle) \quad \text{(forbidden)} , \quad (17c)$$

$$B^- = E_0 + A_h + E(\Gamma_1) + E(|2, \pm 1\rangle) \quad (\sigma) , \quad (17d)$$

$$B^{-\prime} = E_0 + A_h + E(\Gamma_1) + E(|2, 0\rangle) \quad \text{(forbidden)} . \quad (17e)$$

E_0 is the zero-order threefold-degenerate energy state of the bound exciton and corresponds to the absence of intervalley mixing and j-j interaction.

IV. EXPERIMENTAL RESULTS

A. Absorption spectra

1. Zero-stress spectrum

Figure 1 shows the low temperature transmission spectrum obtained from nitrogen-doped gallium phosphide samples. We observe the well-resolved thresholds ($E_{gx} + \mathrm{TA}_X$, $E_{gx} + \mathrm{LA}_X$, $E_{gx} + \mathrm{LO}_X$) corresponding to the intrinsic absorption edge associated with the emission of TA_X, LA_X, and TO_X phonons, respectively. $E_{gx} = 2.330$ eV denotes the excitonic energy gap calculated from the position of the TA_X threshold by taking for the phonon energy $\mathrm{TA}_X = 13.2$ meV (Refs. 29 and 30) or $\mathrm{TA}_X = 13$ meV (Ref. 31). We note that the small A_X structure, previously attributed to the threshold of the free-exciton energy gap, appears to be very close to but not exactly at E_{gx}. At 2.318 eV the spectrum shows the well-known A line associated with the creation of N excitons. The dipole-forbidden B line ($J = 2$ bound-exciton state) does not appear in this low-resolution absorption spectrum. Along with the no-phonon A line, there is a zero-phonon indirect absorption beginining at E_{gx} associated with the free-exciton creation, as well as phonon-induced structures labeled $A + \mathrm{LA}_X$ and $A + \mathrm{TO}_X$. The zero-phonon indirect absorption shows that nitrogen is a very strong perturbation so that it introduces a continuous absorption even above the band gap. This has been studied in detail by Hopfield *et al.*[7] from heavily nitrogen-doped crystals.

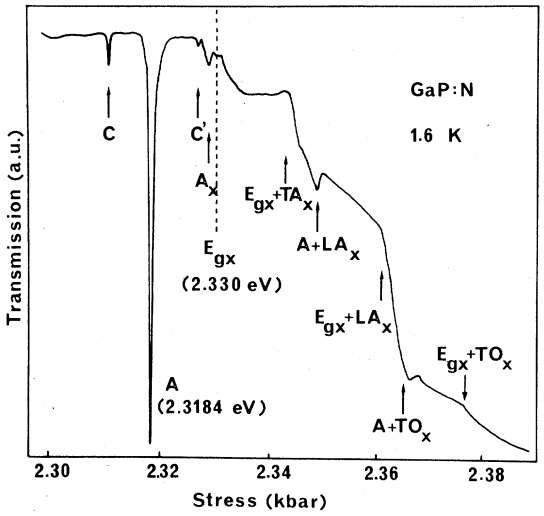

FIG. 1. Typical transmission spectrum obtained at 1.6 K on N-doped GaP sample. The A line corresponds to the creation of the N excitons. The C and C' lines correspond to the creation of S excitons.

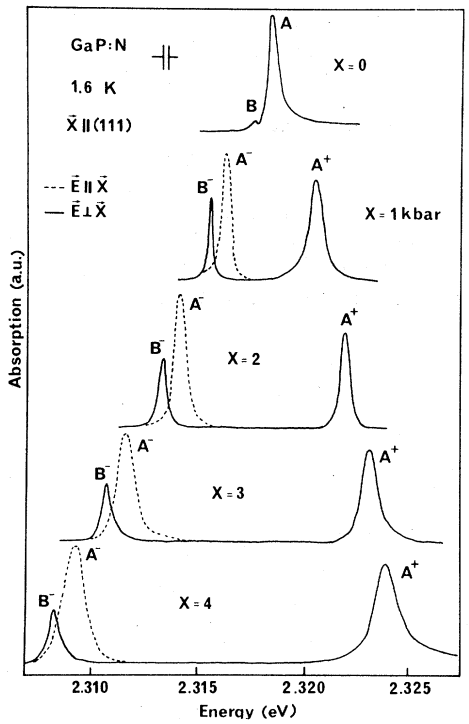

FIG. 2. Effect of a uniaxial stress along the [111] crystallographic direction on the A and B absorption lines. A^+ and B^- appear only with $E \perp X$ (σ polarization). A^- appears only with $E \parallel X$ (π polarization). A^+ is associated with the heavy $|\frac{3}{2}, \frac{3}{2}\rangle$ hole state. A^- and B^- are associated with the light $|\frac{3}{2}, \frac{1}{2}\rangle$ hole state.

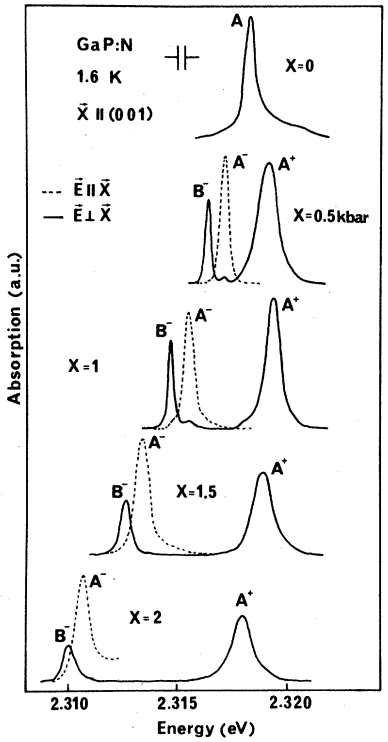

FIG. 3. Effect of a compressive stress along the [001] crystallographic direction.

Finally, the spectrum shows a sharp C line at 2.3108 eV with a small satellite peak C' at 2.327 eV. These lines are associated with the creation of sulfur-bound excitons in the ground and excited states, respectively. The stress behavior of this (D^0X) complex has been analyzed in Refs. 19 and 23 and will not be discussed here.

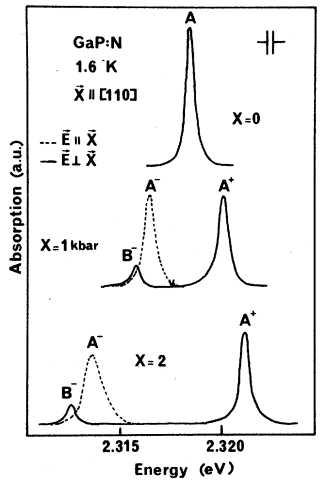

FIG. 4. Effect of a compressive stress along the [110] crystallographic direction.

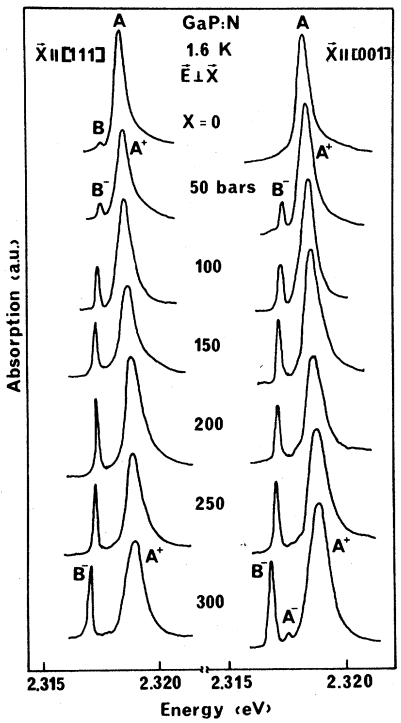

FIG. 5. Effect of very low [111] and [001] compressive stresses on the absorption spectrum in σ polarization. The spectra clearly show the rapid increase of the B^- component which is stress coupled with the A^+ allowed component.

2. *Uniaxial compression*

Absorption spectra from the N excitons are shown in Figs. 2–4 for stress applied along the [111], [001], and [110] axes, respectively. The zero-stress spectra clearly show the A line produced by the excitation of the allowed $J=1$ state. The excitation of the forbidden $J=2$ state, the B

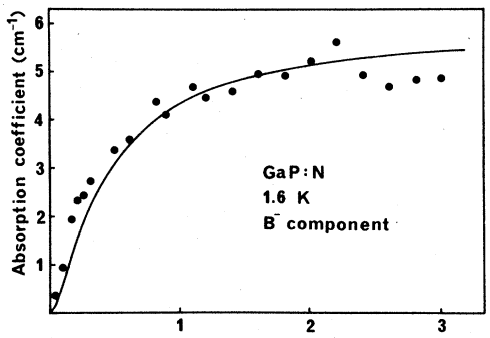

FIG. 6. Comparison of the expected absorption strength of the B^- component in σ polarization with the experimentally observed values, as a function of the applied stress along the [111] crystallographic direction. The calculated values have been adjusted by the factor $\alpha_0 = 24.4\ \text{cm}^{-1}$ [Eq. (19)].

line, occasionally appears weakly in some samples Under stress, the A line splits into two components A^+ and A^-, which appear to be almost totally polarized. This is not in agreement with the group-theory analysis which gives for the A^- line a partial polarization [see Eqs. (17a) and (17b)]. Moreover, the selection rule is stress relaxed and the B^- component of the B line becomes stress allowed. This component is stress coupled with the A^+ component and appears in σ polarization only. Low-stress absorption spectra in σ polarization given in Fig. 5, clearly show the very rapid increase of the B^- component. The strength of the absorption associated with the creation of the $|2,\pm1\rangle$ state (B^- component) is proportional to the square of the amount of the $|1,\pm1\rangle$ state (A^+ component) which its wave function contains. This may be found from

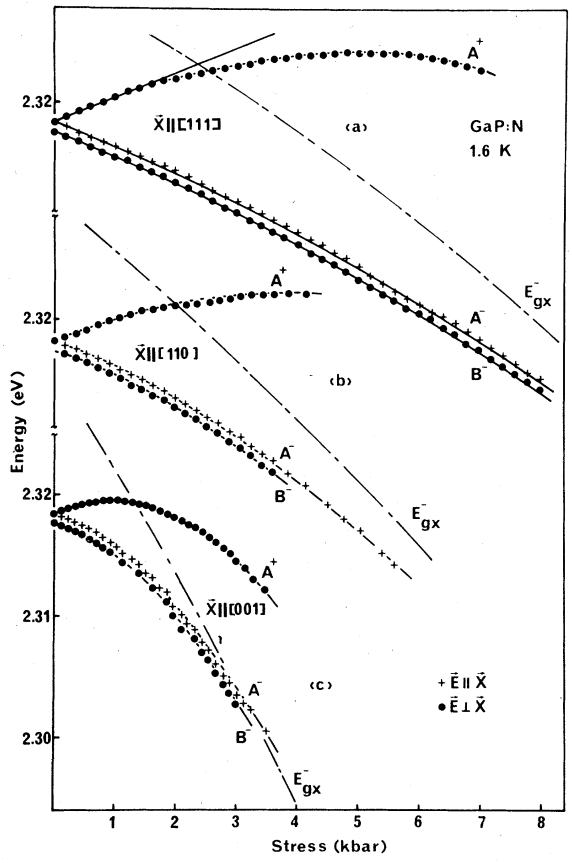

FIG. 7. Uniaxial stress dependence of the A and B exciton-absorption lines with the stress along the [111], [110], and [001] crystallographic directions. The full lines ($X\|[111]$) display the theoretical predictions. They are satisfactorily obeyed by the low-energy components A^- and B^- but fail to explain the nonlinear behavior of the high-energy component A^+. The dashed lines running through the experimental points are guidelines only. The dot-dashed lines show the stress dependence of the low-energy component E_{gx}^- of the indirect free exciton. They are given after the work of Ref. 26.

the eigenvectors of the 2×2 matrix giving rise to the mixing of the $|M|=1$ states[24]:

$$\begin{array}{cc} |1,\pm1\rangle & |2,\pm1\rangle \\ \begin{pmatrix} \frac{5\gamma}{8}+\frac{1}{2}\epsilon & \pm\frac{\sqrt{3}}{2}\epsilon \\ \pm\frac{\sqrt{3}}{2}\epsilon & -\frac{3\gamma}{8}-\frac{1}{2}\epsilon \end{pmatrix} \end{array} . \tag{18}$$

We obtain

$$\alpha=\alpha_0\frac{(E-\frac{5}{8}\gamma-\epsilon/2)^2}{(E-\frac{5}{8}\gamma-\epsilon/2)^2+3\epsilon^2/4}\,, \tag{19}$$

where E is the eigenvalue given by Eq. (14a).

The absorption strength of the B^- component is shown as a function of stress in Fig. 6. The theoretical curve (full line) has been calculated from Eq. (19) with $\gamma=0.91$ meV and $\epsilon=1.94$ meV/kbar. This value of the stress energy is simply the value measured for the free exciton.[26] Taking for the adjustable parameter $\alpha_0=24.4$ cm^{-1}, we obtain a good agreement.

The stress dependence of the absorption lines and the splitting of the $J=1$ state (A^+-A^-) is shown as a function of the applied stress in Figs. 7 and 8, respectively. The following different features have to be considered (i) The shift of the center of gravity of the line (Fig. 7) is much larger for a [001] compression than for a [111] or a [110] compression. (ii) Within the experimental error, the stress splitting (Fig. 8) appears to be isotropic. This result which has already been reported,[21] should be compared with the istropic splittings of the free exciton[26] and of the (D^0X) complex[19] and with the strongly anisotropic splitting of the Bi

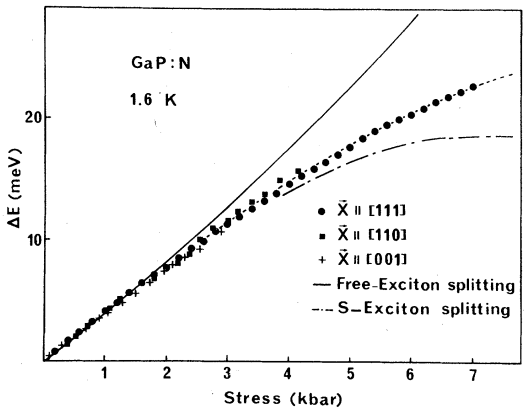

FIG. 8. Stress-induced splitting of the A absorption line. The dashed line is a guideline which illustrates the isotropic behavior of the splitting. For comparison we give the isotropic splitting of the free exciton as obtained in the work of Ref. 26 (full line) and the isotropic splitting of the neutral-donor bound exciton as obtained in the work of Ref. 19 (dot-dashed line).

exciton.[24] It is not surprising since in the N exciton the hole is bound by the long-range Coulomb interaction as it is in the free exciton and in the D^0X complex. On the contrary, in the Bi exciton the hole is bound by the short-range Bi potential.
(iii) All the stress dependences appear to be nonlinear. This is not in agreement with Eqs. (17) which predict a linear [111] stress dependence for the A^+ component. This will be discussed in Sec. V.

B. Luminescence spectra

1. Zero-stress spectrum

Figure 9 shows the low-temperature photoluminescence spectrum obtained from nitrogen-doped gallium phosphide samples excited by the 5145-Å line of the argon laser. The spectrum clearly shows the A-B lines associated with the recombination of the N excitons. At low temperature the low-energy $J=2$ state is much more populated than the high-energy $J=1$ state so that the forbidden transition from the $J=2$ state to the ground state, the B line, can be observed. The J-J splitting A-B is measured to be $\gamma = 0.91$ meV. The A^* and B^* lines correspond to the radiative decay of an excitonic molecule bound to the N trap,[1] the ground states of the transitions being the $J=1$ and $J=2$ states of the single-bound exciton. The stress behavior of the A^* and B^* lines is not reported in the present work.

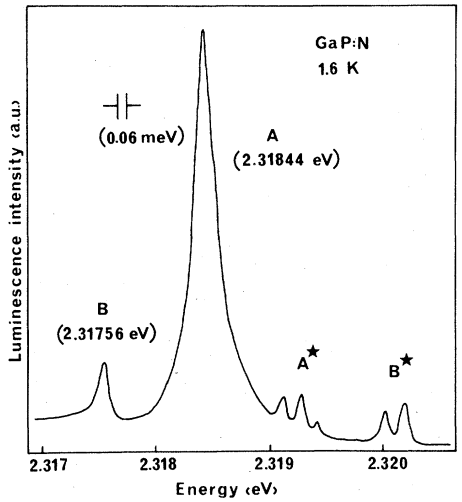

FIG. 9. Photoluminescence spectrum of excitons bound to N in GaP in the region of the no-phonon transitions. The spectrum is taken using the 5145-Å line of the argon laser as exciting wavelength. The A and B lines arise from the decay of the $J=1$ and $J=2$ states of a single exciton bound to nitrogen. The A^* and B^* lines result from the radiative decay of the $J=0$ and $J=2$ (crystal-field split) states of the excitonic molecule bound to nitrogen, the final states of the transitions being the $J=1$ (A line) and $J=2$ (B line) states, respectively, of the single exciton (see Ref. 1).

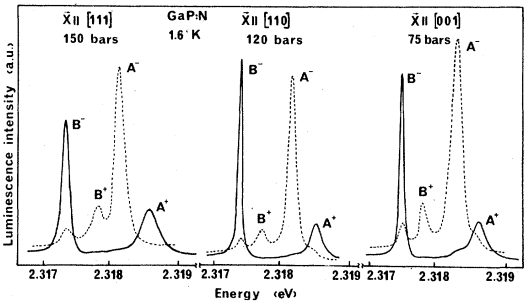

FIG. 10. Effect of a compressive stress along [111], [110], and [001] crystallographic directions on the recombination spectrum of single excitons (A and B lines) bound to nitrogen. (Full line: σ polarization. Dotted line: π polarization.)

2. Uniaxial compression

The effect of a compressive stress along [111], [110], and [001] crystallographic directions on the A and B lines is shown in Fig. 10. The behavior is the same in the three directions. The A line splits into two components A^+ and A^- almost totally polarized. Because of the combined effects of the stress-induced splitting and of the thermalization, the amplitude of the high-energy component A^+ decreases very rapidly with increasing stress, and it could only be resolved up to 1.5 kbar. The B line, weakly allowed at zero-stress, splits into two components B^+ and B^-. The low-energy component B^- is stress coupled with the A^+ component and becomes stress allowed in σ polarization. In π polarization this component should be dipole forbidden. The high-energy component B^+ should be also dipole forbidden in all polarizations. In fact, both B^- and B^+ appear weakly in π polarization but this breaking of the selection rules is not related to the external stress. It depends on the same mechanism which renders the B line weakly allowed at zero stress (see Fig. 9).

The stress dependence and the splitting of the A and B lines are shown as a function of the applied stress in Figs. 12–14 and will be analyzed in Sec. V B.

V. ANALYSIS OF THE DATA

A. High-stress behavior

The high-stress behavior is given experimentally by the absorption data and theoretically by Eqs. (17) where the stress dependences of the $|J,M\rangle$ states are given by Eqs. (15).

1. [111] stress

The three minima of the conduction band remain equivalent and the only shear dependence comes from the Γ_8-like bound hole. The stress dependences of A^+, A^-, and B^-, calculated from Eqs.

(17), (16a), and (15) are then given by

$$A^+ = E_0 - 2\Delta + \tfrac{3}{8}\gamma + A_h + \epsilon\,, \tag{20a}$$

$$A^- = E_0 - 2\Delta + \tfrac{5}{8}\gamma + A_h - \epsilon - 2\epsilon'^2/(\Delta_0 + \epsilon)\,, \tag{20b}$$

$$B^- = E_0 - 2\Delta - \tfrac{1}{8}\gamma + A_h - \epsilon - 2\epsilon'^2/(\Delta_0 + \epsilon)\,. \tag{20c}$$

Using the low-temperature values of the elastic compliance constants S_{ij} of GaP,[32] together with the shear deformation potentials d and d' and the spin-orbit parameter Δ_0 obtained in pure GaP,[26] we obtain the best fit with the experimental points by using for A_h the value $A_h = 0.1 \pm 0.1$ meV/kbar. This value is very close to the one reported by Merz *et al.*[20] This gives for the hydrostatic deformation potential of the bound exciton the value $a = -0.3 \pm 0.3$ eV which is to be compared with the corresponding value for the free exciton[26] and the (D^0X) complex[19] 2.3 eV. This will be discussed in Sec. VI. The calculated stress dependences of A^+, A^-, and B^- are given as full lines in Fig. 7(a). We note the satisfactory agreements obtained over the full experimental range for the low-energy components A^- and B^- but only up to about 2 kbar for the high-energy A^+ component. This unexpected nonlinear behavior [see Eq. (20a)] of the high-energy component has already been observed[19] and explained[23] for the (D^0X) complex. It is not related to a nonlinear shift of the partner electron of the bound exciton but to a behavior of the A^+ component as a whole. This behavior is believed to result from the stress-induced coupling of A^+ with low-energy subcomponents of the stress-split excited states ($n = 2$) of the bound exciton. A crude estimate of this stress-induced admixture may be obtained from the nonlinear part of the energy shift of A^+. We obtain for the zero-stress energy of the excited state involved, $E \simeq 2.355 \pm 0.005$ eV, and for the interaction energy $\delta \simeq 10 \pm 5$ meV.

2. *[001] and [110] stresses*

An axial stress in the [001] or [110] direction lifts the degeneracy of the three conduction-band valleys and changes the energy of the valley-orbit split states. The energy shift $E(\Gamma_1)$ [Eq. (16a)] is then nonlinear and gives rise to a nonlinear energy displacement of the center of gravity of the bound-exciton lines. This is illustrated in Fig. 7, where we find a much larger shift in configuration $X \parallel [001]$ then we do in configuration $X \parallel [110]$ and $X \parallel [111]$, respectively. In order to obtain the valley-orbit coupling matrix element Δ, we must extract the shear dependence $E(\Gamma_1)$ from the resulting stress dependence of the exciton state. This is done in the following way: The stress-induced splitting of the A line has been found to be isotropic (Fig. 8) and, consequently, in Eqs. (17) the $E(|J,M\rangle)$ terms are isotropic. The only terms which depend on the direction of the applied stress are $E(\Gamma_1)$. Then we can write

$$A^-_{001} - A^-_{111} = E(\Gamma_1)_{001} - E(\Gamma_1)_{111} = \tfrac{1}{2}\Delta[3 + x - 3(1 + \tfrac{2}{3}x + x^2)^{1/2}]\,. \tag{21}$$

In the same manner,

$$A^-_{110} - A^-_{111} = E(\Gamma_1)_{110} - E(\Gamma_1)_{111}\,.$$

The experimental results are given in Fig. 11. The full and dotted lines correspond to the calculated curves [Eq. (21)] using for the shear deformation potential E_2 the value 6.9 eV which corresponds, within the experimental error, to the value measured for the free excitons.[26] The best fit is obtained by using a stress-dependent value of the intervalley-coupling matrix element Δ given by

$$\Delta(X) = \Delta + kX\ (\text{kbar})\,.$$

We find $\Delta = 8$ meV and $k = 0.4$ meV/kbar. X is negative for a compression.

The zero-stress value $\Delta = 8$ meV gives for the valley-orbit splitting of the bound exciton the value $E_{12} = 24$ meV. It is to be noted that this value confirms that the first excited state of the N exciton is degenerated with the free-exciton continuum. This result is in agreement with the calculations of Faulkner[15] and of Jaros *et al.*[17]

B. Low-stress behavior

The low-stress behavior is given experimentally by the high-resolution luminescence data and theoretically by Eqs. (17), (16a), and (14). The results are shown in Figs. 12–14 for the [111], [110], and [001] stress directions, respectively.

It is to be noted that, on account of the relative magnitudes of the j-j splitting ($\gamma = 0.9$ meV) and of the stress-induced valence-band splitting ($2\epsilon = 3.9$ meV/kbar), the nonlinear behavior resulting from the stress-induced mixing of the $|J,M\rangle$ states could only have been observed under very low stress conditions, typically $X < 200$ bar. Since the energy of the luminescence lines is a function of the stress produced near the sample surface and since it is very difficult to measure with sufficient accuracy the very small uniaxial surface stress used in the present study, we have used as a strain gauge the energy of the $|1,0\rangle$ exciton state (A^- line) which is not stress-mixed with another $|J,M\rangle$ state.

The solid lines in Figs. 12–14 correspond to the theoretical calculation [Eqs. (17), (16a), and (14)], using for the different parameters the values deduced from the absorption data. For all stress directions we note a very satisfactory agreement between the experimental and calculated results.

Finally, we note an important result. In all

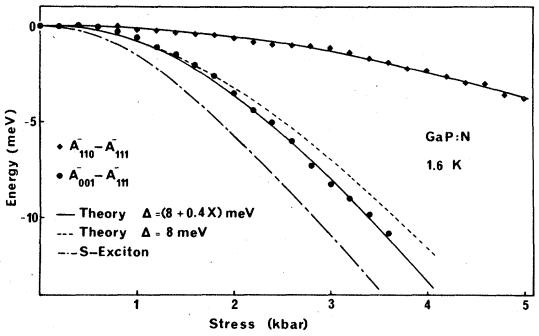

FIG. 11. Shear dependence of the bound-electron ground state (Γ_1). The calculated curves correspond to an intervalley-coupling matrix element: $\Delta(X) = (8 + 0.4\,X)$ meV (X is expressed in kbar and is negative for a compression).

stress directions the high-energy component B^+ exhibits a nearly linear behavior in agreement with the isotropic-coupling theory presented in Sec. III. This results from the isotropic splitting of the hole states which has already been reported in Fig. 8. The effect of an anisotropic splitting of the hole states has been clearly discussed by Onton and Morgan[24] which show that this anisotropy gives rise to a stress-induced coupling between the A^- allowed component and the B^+ forbidden one under

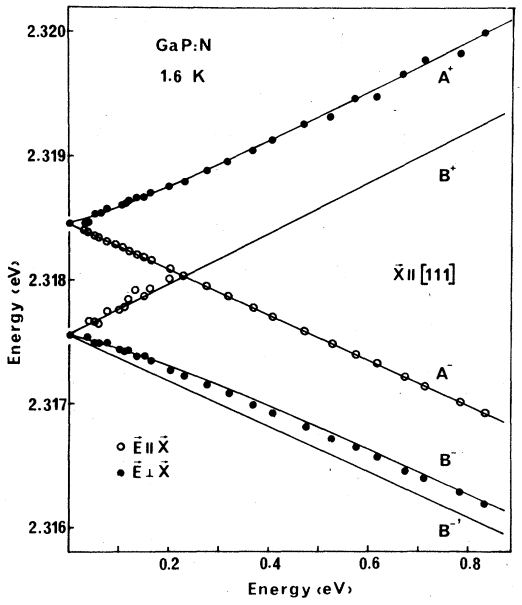

FIG. 12. Stress dependence of the A and B exciton recombination lines with low stress along the [111] crystallographic direction. The data were taken at 1.6 K. The full lines are calculated with Eqs. (17), (16a), and (14). The parameters used for the calculation are deduced from absorption data. In this figure, the energy of the $|10\rangle$ exciton state (A^- line) which is not stress mixed, has been taken as the strain gauge.

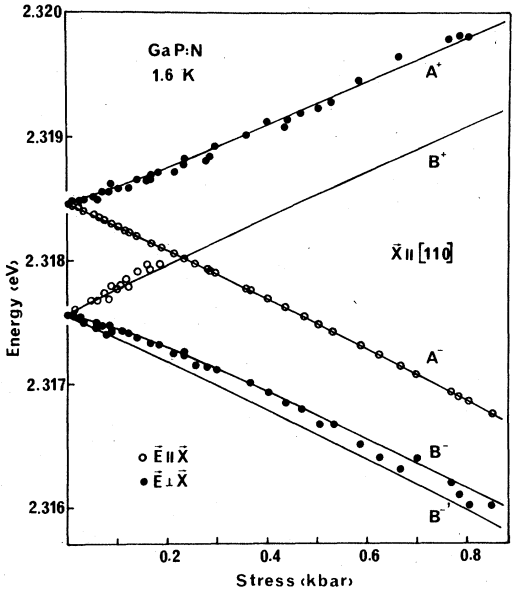

FIG. 13. Same as Fig. 11 with $X \parallel [110]$.

[110] stress [see Eq. (B17) in Ref. 24]. As a consequence of this coupling, the [110] stress behavior of the B^+ component should exhibit (i) a nonlinear stress dependence and (ii) an oscillator strength increasing with stress. This does not agree with the experimental results: (i) The stress dependence appears to be nearly linear up to $A^- - B^+ = 0.1$ meV (Fig. 13). (ii) The oscillator strength appears to be independent of the stress. This is shown in Fig. 15 where there are several photoluminescence spectra given from $X = 0$ to

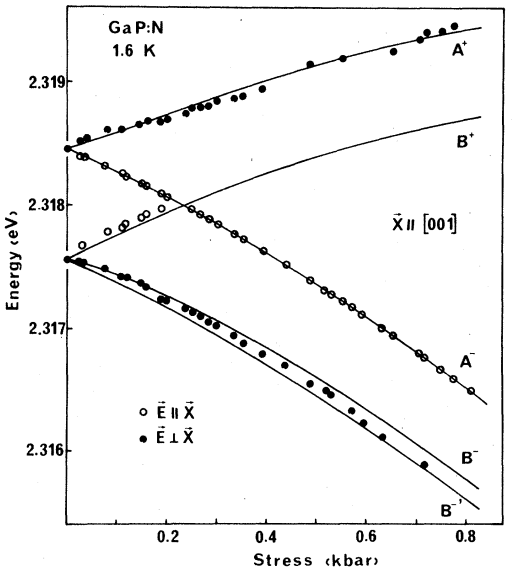

FIG. 14. Same as Fig. 11 with $X \parallel [001]$.

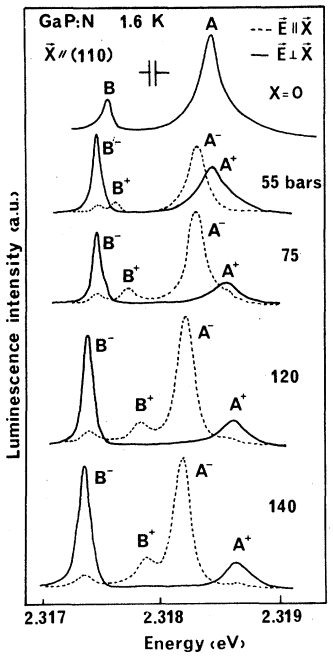

FIG. 15. Effect of a very low [110] compressive stress on the oscillator strength associated with the recombination of the $|2,\pm2\rangle$ exciton state (B^+ line). The spectra clearly show that the amplitude of the B^+ component remains constant when going toward the A^- component. These two components do not appear to be stress coupled.

140 bar.

In summary, both the high-stress behavior (absorption) and the low-stress behavior (luminescence) are in agreement with an isotropic splitting of the bound-hole state in the N exciton. This is not the case for the Bi exciton.[24]

VI. DISCUSSION

We will discuss in this section some important results.

(i) The [111], [110], and [001] stress-directions give rise to stress dependences which are strongly different (Fig. 7). A strong valley-repopulation effect appears for the [001] stress, while the [111] stress dependence is very well accounted for by Eqs. (20) without any valley-repopulation effect. This result is in agreement with the recent calculations of Jaros and Brand.[17] The computed composition of the wave function, i.e., the coefficients A_{nk} [Eqs. (2)–(15) in Ref. 17], shows that most of the coefficients are very small except those located near Γ-X line in the Brillouin zone. Moreover, while the states of X_1 and Γ_1 conduction-band valleys have large wave-function coefficients (see Table I of Ref. 17), it is not the same for the L_1 valley.

(ii) We measure $\Delta = 8$ meV. It is worth noting that this value has the same order of magnitude as the one obtained for the (D^0X) complex in GaP:S,[19] $\Delta_s = 4$ meV. This result is surprising on account of the difference between the short-range nitrogen potential and the long-range Coulomb sulfur potential. Now, if the theory as given applies very well to the case of the (D^0X) complex, its applicability to the case of the N exciton is not obvious for two reasons. First, the N-exciton wave function does not contain X_1 Bloch states only. Second, the Γ_{12} state appears to be a resonant state above the free exciton, so that it is presumably mixed with many Γ_{12} states with free-exciton character. As a consequence, the parameters Δ_s and Δ_N must be compared with caution.

(iii) Another important feature, which has already been reported,[20] concerns the stress dependence of the binding energy of the N exciton. The hydrostatic component of the shift of the bound exciton is $A_h = +0.1 \pm 0.1$ meV/kbar, while the corresponding parameter for the free exciton has been found[26] to be $A_x = -0.85 \pm 0.20$ meV/kbar. The binding energy of the bound exciton is thus stress dependent with a hydrostatic coefficient of about -1 meV/kbar, which corresponds to the hydrostatic pressure coefficient $dE_b/dP = -3$ meV/kbar. This stress-dependent binding energy must be compared with the composition-dependent binding energy of the N exciton in $GaAs_{1-x}P_x$:N.[6-13] The stress (composition) dependence of E_b results from the stress (composition) dependence of the conduction-band structure and/or the nitrogen potential. In the case of $GaAs_{1-x}P_x$:N it has been shown[12,13] that the x dependence of the potential plays the main part in the x dependence of E_b.

In the same way, the stress dependence of the potential plays the main part in the stress dependence of E_b for two different reasons:

(a) We have calculated the effect on E_b of the stress dependence of the conduction band by considering three regions in the Brillouin zone, namely, X, L, and Γ, each subzone being assumed to shift differently under stress. The result (see the Appendix) clearly shows that a combined X-L nature of the wave function of the bound electron, if it exists, does not explain the stress dependence of E_b.

(b) On the other hand, the intervalley-coupling matrix element Δ has been found to be stress dependent. This result clearly shows that the nitrogen potential is stress dependent. Both the zero-order energy state E_0 and the intervalley coupling Δ are then stress dependent so that the variation of the binding energy of the exciton is given by

$$\frac{dE_b}{dX}=\frac{dE_0}{dX}+2\frac{d\Delta}{dX}.$$

We have measured $dE_b/dX=1$ meV/kbar and $d\Delta/dX=0.4$ meV/kbar, so that almost all the stress dependence of E_b may be accounted for by the stress dependence of the intervalley coupling. Using a Gaussian potential, Faulkner[15] has reported that the intervalley coupling Δ is very sensitive to the range of the potential. The decrease of Δ under compression is then believed to result mainly from the decrease of the lattice constant, giving rise to a relative increase of the range of the nitrogen potential. Δ, which is very sensitive to the range of the potential, may be used to check how short the potential range is. Using the results reported by Faulkner[15] for a Gaussian potential of extension $A=\alpha a$ (where a is the lattice constant), we may estimate the value of α to be $\simeq 0.95 \pm 0.05$.

VII. CONCLUSION

We have investigated the uniaxial dependence of the N excitons GaP. The low-stress behavior of the exciton states is consistent with the simple j-j coupling model for the exciton. The high-stress behavior is consistent with an exciton wave function located at the X point; the valley-repopulation effect is only observed for [110] and [001] stresses. The valley-orbit splitting is measured to be $E_{12}=24$ meV. This value corresponds with an unbounded Γ_{12} valley-orbit split state, in agreement with Faulkner's calculations.[15] On the other hand, the valley-orbit coupling matrix element Δ appears to be stress dependent. This dependence is believed to result mainly from the stress dependence of the potential range. Finally, in the model of a Gaussian potential, the range A is estimated to be 0.95 ± 0.05 in units of the lattice constant.

ACKNOWLEDGMENTS

We greatly thank Dr. Poiblaud and the Radiotechnique-Compelec (Caen, France) for kindly providing us with the GaP samples used in the experiment. We also thank Professor F. Bassani for helpful discussions.

APPENDIX

In order to calculate the effect of the stress dependence of the conduction-band structure, we consider three regions in the Brillouin zone, namely, X, L, and Γ, each subzone having been assumed to shift rigidly under stress. The coupled-valleys matrix is written

$$\begin{array}{c|cccccccc}
 & |\phi^0\rangle_{100} & |\phi^0\rangle_{010} & |\phi^0\rangle_{001} & |\phi^0\rangle_{111} & |\phi^0\rangle_{\bar{1}11} & |\phi^0\rangle_{1\bar{1}1} & |\phi^0\rangle_{11\bar{1}} & |\phi^0\rangle_{000} \\
\hline
 & E_X^0+A_X+2\Delta x & -\Delta & -\Delta & -\delta & -\delta & -\delta & -\delta & -\delta' \\
 & -\Delta & E_X^0+A_X-\Delta x & -\Delta & -\delta & -\delta & -\delta & -\delta & -\delta' \\
 & -\Delta & -\Delta & E_X^0+A_X-\Delta x & -\delta & -\delta & -\delta & -\delta & -\delta' \\
 & -\delta & -\delta & -\delta & E_L^0+A_L+3\Delta' y & -\Delta' & -\Delta' & -\Delta' & -\delta'' \\
 & -\delta & -\delta & -\delta & -\Delta' & E_L^0+A_L-\Delta' y & -\Delta' & -\Delta' & -\delta'' \\
 & -\delta & -\delta & -\delta & -\Delta' & -\Delta' & E_L^0+A_L-\Delta' y & -\Delta' & -\delta'' \\
 & -\delta & -\delta & -\delta & -\Delta' & -\Delta' & -\Delta' & E_L^0+A_L-\Delta' y & -\delta'' \\
 & -\delta' & -\delta' & -\delta' & -\delta'' & -\delta'' & -\delta'' & -\delta'' & E_\Gamma^0+A_\Gamma
\end{array} \qquad \text{(A1)}$$

In the matrix equation (A1), $E^0_{X,L,\Gamma}$ are the zero-order energy states associated with the X, L, and Γ subzones, respectively. Δ, Δ', δ, δ', and δ'' are the X-X, L-L, X-L, X-Γ, and L-Γ intervalley couplings, respectively. A_X, A_L, and A_Γ are the hydrostatic components of the energy shifts of the X, L, and Γ minima, respectively. The shear dependences of the X and L valleys are given by the parameters x and y which are given by $x=E_2S/6\Delta$, $y=E_2'S'/9\Delta'$. E_2 and E_2' are the shear deformation potentials of the X and L valleys, respectively. S is given in Table I for different stress directions and S' is given by $S'=S_{44}X$ for $X\|[111]$, $S'=-S_{44}X$ for $X\|[110]$, and $S'=0$ for $X\|[001]$.

It is worth noting that, in order to reduce the order of the matrix (A1) we have used symmetric combinations of the wave functions associated with the L valleys, namely, $|\phi^0\rangle_{111}=(1/\sqrt{2})(|\phi^0\rangle_{111}+|\phi^0\rangle_{\bar{1}\bar{1}\bar{1}})$, so that $\delta=\frac{1}{2}(\delta_a+\delta_0)$, where a means adjacent and refers to the smallest $|k_i-k_j|$ between X and L minima, and 0 means opposite and refers to the largest $|k_i-k_j|$.

Now, in the basis which diagonalizes the 3×3 and 4×4 matrix separately, the matrix equation (A1) becomes

$$
\begin{array}{c|cccccccc}
 & |\Gamma_1\rangle_X & |\Gamma_{12}^a\rangle_X & |\Gamma_{12}^b\rangle_X & |\Gamma_1\rangle_L & |\Gamma_{15}^x\rangle_L & |\Gamma_{15}^y\rangle_L & |\Gamma_{15}^z\rangle_L & |\Gamma_1\rangle_\Gamma \\
\hline
|\Gamma_1\rangle_X & E_X^0+A_X+E(\Gamma_1)_X & 0 & 0 & -\frac{\sqrt{3}(b+3)}{[(1+a^2)(3+b^2)]^{1/2}}\delta & -\frac{3(b-1)}{(3+b^2)^{1/2}}\delta & 0 & 0 & -\frac{\sqrt{3}}{(1+a^2)^{1/2}}\delta' \\
|\Gamma_{12}^a\rangle_X & 0 & E_X^0+A_X+E(\Gamma_{12}^a) & 0 & -\frac{2a\sqrt{3}}{(1+a^2)^{1/2}}\delta & 0 & 0 & 0 & -\frac{a\sqrt{3}}{(1+a^2)^{1/2}}\delta' \\
|\Gamma_{12}^b\rangle_X & 0 & 0 & E_X^0+A_X+\Delta(1-x) & 0 & 0 & 0 & 0 & 0 \\
|\Gamma_1\rangle_L & -\frac{\sqrt{3}(b+3)}{[(1+a^2)(3+b^2)]^{1/2}}\delta & -\frac{2a\sqrt{3}}{(1+a^2)^{1/2}}\delta & 0 & E_L^0+A_L+E(\Gamma_1)_L & 0 & 0 & 0 & -\frac{3+b}{(3+b^2)^{1/2}}\delta'' \\
|\Gamma_{15}^x\rangle_L & -\frac{3(b-1)}{(3+b^2)^{1/2}}\delta & 0 & 0 & 0 & E_L^0+A_L+E(\Gamma_{15}^x)_L & 0 & 0 & -\frac{\sqrt{3}(b-1)}{(3+b^2)^{1/2}}\delta'' \\
|\Gamma_{15}^y\rangle_L & 0 & 0 & 0 & 0 & 0 & E_L^0+A_L+\Delta'(1-y) & 0 & 0 \\
|\Gamma_{15}^z\rangle_L & 0 & 0 & 0 & 0 & 0 & 0 & E_L^0+A_L+\Delta'(1-y) & 0 \\
|\Gamma_1\rangle_\Gamma & -\frac{\sqrt{3}}{(1+a^2)^{1/2}}\delta' & -\frac{a\sqrt{3}}{(1+a^2)^{1/2}}\delta' & 0 & -\frac{3+b}{(3+b^2)^{1/2}}\delta'' & -\frac{\sqrt{3}(b-1)}{(3+b^2)^{1/2}}\delta'' & 0 & 0 & E_\Gamma^0+A_\Gamma
\end{array}
\tag{A2}
$$

where $E(\Gamma_1)_X$ and $E(\Gamma_{12}^a)$ are given by Eqs. (16a) and (16b), respectively,

$$E(\Gamma_1)_L = \Delta'[-1+y-2(1+y+y^2)^{1/2}] ,$$

$$E(\Gamma_{15}^x) = \Delta'[-1+y+2(1+y+y^2)^{1/2}] ,$$

$$a = \frac{-x\sqrt{2}}{1+x+3(1+\frac{2}{3}x+x^2)^{1/2}} ,$$

$$b = -1-2y+2(1+y+y^2)^{1/2} .$$

The [111] stress corresponds to $a=0$, and the [001] stress corresponds to $b=1$.

The wave functions of the new basis are[33]

$$|\Gamma_1\rangle_X = \frac{1}{\sqrt{6}}\frac{1}{(1+a^2)^{1/2}}(\sqrt{2}+a, \sqrt{2}+a, \sqrt{2}-2a) ,$$

$$|\Gamma_{12}^a\rangle = \frac{1}{\sqrt{6}}\frac{1}{(1+a^2)^{1/2}}(a\sqrt{2}-1, a\sqrt{2}-1, a\sqrt{2}+2) ,$$

$$|\Gamma_{12}^b\rangle = \frac{1}{\sqrt{2}}(1, \bar{1}, 0) ,$$

$$|\Gamma_1\rangle_L = \frac{1}{(3+b^2)^{1/2}}(b, 1, 1, 1) ,$$

$$|\Gamma_{15}^x\rangle = \frac{1}{\sqrt{3}}\frac{b}{(3+b^2)^{1/2}}\left(-\frac{3}{b}, 1, 1, 1\right) ,$$

$$|\Gamma_{15}^y\rangle = \frac{1}{\sqrt{2}}(0, 1, 0, \bar{1}) ,$$

$$|\Gamma_{15}^z\rangle = \frac{1}{\sqrt{6}}(0, 1, \bar{2}, 1) .$$

In order to investigate the stress dependence of the $|\Gamma_1\rangle_X$ ground state, let us first consider the effect of a hydrostatic pressure. In this case $x=y=0$ so that $a=0$ and $b=1$, and the stress dependence of a given subzone reduces to $3A_{X,L,\Gamma}$. The stress dependence of the $|\Gamma_1\rangle_X$ state is then an eigenvalue of the following 3×3 matrix:

$$
\begin{array}{c}
\begin{array}{ccc} |\Gamma_1\rangle_X & |\Gamma_1\rangle_L & |\Gamma_1\rangle_\Gamma \end{array} \\
\begin{pmatrix} E_X^0-2\Delta+3A_X & -2\sqrt{3}\,\delta & -\sqrt{3}\,\delta' \\ -2\sqrt{3}\,\delta & E_L^0-3\Delta'+3A_L & -2\delta'' \\ -\sqrt{3}\delta' & -2\delta'' & E_\Gamma^0+3A_\Gamma \end{pmatrix}
\end{array} . \tag{A3}
$$

Now the energy differences $(E_L^0-E_X^0)$ and $(E_\Gamma^0-E_X^0)$ are 300 (Ref. 34) and 500 meV (Ref. 26), respectively. Moreover the density of states is much more important at the L subzone than at the Γ subzone. As a consequence, the eigenvalues of Eq. (A3) can be found by first diagonalizing the 2×2 matrix in the upper-left-hand corner and then including the effects of the $|\Gamma_1\rangle_\Gamma$ state as a perturbation. Taking account of the relative order of magnitude of δ and $E_L^0-E_X^0$ and neglecting to a first approximation the effect of the $|\Gamma_1\rangle_\Gamma$ state, the pressure dependence of the $|\Gamma_1\rangle$ ground state is given by

$$\frac{dE(|\Gamma_1\rangle)}{dP}=3\left(1-\frac{3\delta^2}{(E_X^0-E_L^0)^2}\right)A_X+3\frac{3\delta^2}{(E_X^0-E_L^0)^2}A_L\,. \quad \text{(A4)}$$

Using $E_X^0-E_L^0=300$ meV, $A_X=-0.85$ meV/kbar,[26] $A_L=1.67$ mev/kbar (value measured on germanium[35]), and for the hydrostatic coefficient the measured value $dE\,(|\Gamma_1\rangle)/dP=3\,A_h$, we obtain $\delta=53$ meV.

This value must be compared with $\Delta=8$ meV and appears to be unrealistic. Nevertheless it corresponds with a wave function of the resulting ground state given by

$$|\Gamma_1\rangle=0.95\,|\Gamma_1\rangle_X+0.30\,|\Gamma_1\rangle_L\,. \quad \text{(A5)}$$

Although this result is unlikely, it cannot be ruled out so that the result of hydrostatic pressure measurements does not permit us to tell if the stress dependence of the band structure is or is not the reason of the stress dependence of the exciton binding energy.

Let us now consider the case of uniaxial stress, and more particularly a [111] stress. In this case $a=x=0$ and the stress dependence of the $|\Gamma\rangle_X$ state is given by the diagonalization of the matrix equation (A6):

$$\begin{array}{c} \begin{matrix} |\Gamma_1\rangle_X & |\Gamma_1\rangle_L & |\Gamma_{15}^x\rangle_L & |\Gamma_1\rangle_\Gamma \end{matrix} \\ \begin{pmatrix} E_X^0+A_X & -\frac{\sqrt{3}\,(3+b)}{(3+b^2)^{1/2}}\delta & -\frac{3(b-1)}{(3+b^2)^{1/2}}\delta & -\sqrt{3}\,\delta' \\ -\frac{\sqrt{3}\,(3+b)}{(3+b^2)^{1/2}}\delta & E_L^0+A_L+E(\Gamma_1)_L & 0 & -\frac{3+b}{(3+b^2)^{1/2}}\delta'' \\ -\frac{3(b-1)}{(3+b^2)^{1/2}}\delta & 0 & E_L^0+A_L+E(\Gamma_{15}^x) & -\frac{\sqrt{3}(b-1)}{(3+b^2)^{1/2}}\delta'' \\ -\sqrt{3}\,\delta' & -\frac{3+b}{(3+b^2)^{1/2}}\delta'' & -\frac{\sqrt{3}\,(b-1)}{(3+b^2)^{1/2}}\delta'' & E_\Gamma^0+A_\Gamma \end{pmatrix} \end{array} . \quad \text{(A6)}$$

Let us consider a new basis with the symmetric and antisymmetric combinations of the wave function associated with the L minima:

$$|\Gamma^{\pm}\rangle_L=(1/\sqrt{2})(|\Gamma_1\rangle_L\pm|\Gamma_{15}^x\rangle_L)\,. \quad \text{(A7)}$$

We obtain the matrix equation (A8):

$$\begin{array}{c} \begin{matrix} |\Gamma_1\rangle_X & |\Gamma^+\rangle_L & |\Gamma^-\rangle_L & |\Gamma_1\rangle_\Gamma \end{matrix} \\ \begin{pmatrix} E_X^0+A_X & -\sqrt{3}\,\delta^+ & -\sqrt{3}\,\delta^- & -\sqrt{3}\,\delta' \\ -\sqrt{3}\,\delta^+ & E_L^0+A_L-\Delta'(1-y) & -2(1+y+y^2)^{1/2} & -\delta^+ \\ -\sqrt{3}\,\delta^- & -2(1+y+y^2)^{1/2} & E_L^0+A_L-\Delta'(1-y) & -\delta^- \\ -\sqrt{3}\,\delta' & -\delta^+ & -\delta^- & E_\Gamma^0+A_\Gamma \end{pmatrix} \end{array} , \quad \text{(A8)}$$

with

$$\delta^{\pm}=[\delta/\sqrt{2}\,(3+b^2)^{1/2}][(3+b)\pm\sqrt{3}\,(b-1)]\,.$$

Neglecting in first approximation the effect of the $|\Gamma_1\rangle_\Gamma$ state compared to that of one of the $|\Gamma_L\rangle$ states, we consider the 3×3 matrix in the upper-left-hand corner. This matrix couples three states whose diagonal stress dependences are A_X for the first one and $A_L+\Delta' y$ for the second and third ones. Now we wish to compare the numerical values. A_X has been measured to be -0.85 meV/kbar; $A_L+\Delta' y=A_L+E_2'S'/9$. Using $A_L=1.67$ meV/kbar (Ref. 35) and $E_2'=16$ eV (Ref. 36), which are the values measured on germanium, we calculate $A_L+\Delta' y=-0.82$ meV/kbar. The three coupled states $|\Gamma_1\rangle_X$, $|\Gamma^+\rangle_L$, and $|\Gamma^-\rangle_L$ have then the same stress dependence. Consequently their coupling does not permit us to explain the observed stress dependence, $A_h=+0.1$ meV/kbar, for the bound-exciton ground state.

Last but not least, a consequence of the subsidiary valley admixtures with their own valley-repopulation effect would be to change the calculated hydrostatic component of the uniaxial-stress dependence. In other words, a [111] uniaxial stress does not lift the degeneracy of the three X valleys, thus producing no repopulation effect and giving rise to the linear hydrostatic component A_h. Now the introduction of L valleys would introduce a small valley-repopulation effect similar to the one found for the $1s$-A donor state in germanium and would produce a small nonlinear behavior of A_h. This is not found experimentally; all repopulation effects are restricted to [001] and [110] stress directions.

In summary, the uniaxial-stress data clearly show that the hydrostatic component of the stress dependence, and consequently the pressure coefficient, of the binding energy E_b of the N exciton is not accounted for by the stress dependence of the conduction-band structure.

---

*Permanent address: Dept. Electricitat i Electronica, Universitat Autonoma de Barcelona, Bellaterra, Barcelona, Spain.
†Centre associé au CNRS.

[1]J. L. Merz, R. A. Faulkner, and P. J. Dean, Phys. Rev. 188, 1228 (1969).
[2]P. J. Dean, J. Lumin. 12, 398 (1970).
[3]Y. Kaifu, T. Komatsu, and Y. Takimura, J. Phys. Soc. Jpn. 38, 791 (1975).
[4]R. A. Street and P. J. Wiesner, Phys. Rev. B 14, 632 (1976).
[5]E. Cohen and M. D. Sturge, Phys. Rev. B 15, 1039 (1977).
[6]D. R. Scifres, N. Holonyak, Jr., C. B. Duke, G. G. Kleiman, A. B. Kunz, M. G. Craford, W. O. Groves, and A. H. Herzog, Phys. Rev. Lett. 27, 191 (1971).
[7]J. J. Hopfield, P. J. Dean, and D. G. Thomas, Phys. Rev. 158, 748 (1967).
[8]D. E. Aspnes, C. G. Olson, and D. W. Lynch, Phys. Rev. Lett. 37, 766 (1976).
[9]D. E. Aspnes, Phys. Rev. B 14, 5331 (1976).
[10]G. G. Kleiman, R. J. Nelson, N. Holonyak, Jr., and J. J. Coleman, Phys. Rev. Lett. 37, 375 (1976).
[11]G. G. Kleiman, Phys. Rev. B 15, 802 (1977).
[12]W. Y. Hsu, J. D. Dow, D. J. Wolford, and B. G. Streetman, Phys. Rev. B 16, 1597 (1977).
[13]G. G. Kleiman and M. F. Decker, Phys. Rev. B 17, 924 (1978).
[14]P. J. Dean and D. C. Herbert, in *Excitons*, edited by K. Cho (Springer, New York, 1979), p. 55.
[15]R. A. Faulkner, Phys. Rev. 175, 991 (1968).
[16]J. W. Allen, J. Phys. C 1, 1136 (1968); 4, 1936 (1971).
[17]M. Jaros and S. Brand, J. Phys. C 12, 525 (1979), and references therein.
[18]D. D. Manchon and P. J. Dean, *International Conference on the Physics of Semiconductors, Cambridge, 1970,* edited by Seymour P. Keller, J. C. Hensel, and F. Stern.
[19]H. Mathieu, B. Archilla, P. Merle, and J. Camassel, Phys. Rev. B 20, 4268 (1979).
[20]J. L. Merz, A. Baldereschi, and A. M. Sergent, Phys. Rev. B 6, 3082 (1972).
[21]F. H. Pollak, P. M. Raccah, R. S. Bauer, and R. D. Burnham, Nuovo Cimento 39B, 437 (1977).
[22]F. Bassani, G. Iadonisi, and B. Presiozi, Rep. Prog. Phys. 37, 1099 (1974).
[23]H. Mathieu, J. Camassel, and P. Merle, Phys. Rev. B 21, 2466 (1980).
[24]A. Onton and T. N. Morgan, Phys. Rev. B 1, 2592 (1970).
[25]J. V. W. Morgan and T. N. Morgan, Phys. Rev. B 1, 739 (1970).
[26]H. Mathieu, P. Merle, E. L. Ameziane, B. Archilla, J. Camassel, and G. Poiblaud, Phys. Rev. B 19, 2209 (1979).
[27]P. Price, Phys. Rev. 104, 1223 (1956).
[28]D. K. Wilson and G. Feher, Phys. Rev. 124, 1068 (1961).
[29]J. L. Yarnell, J. L. Warren, R. G. Kenzel, and P. J. Dean, *The Fourth* IAEA *Symposium on Neutron Inelastic Scattering, Copenhagen, Denmark, 1968* (IAEA, Vienna, 1968), Vol. I, p. 301.
[30]E. S. Koteles and W. R. Datars, Solid State Commun. 19, 221 (1976).
[31]D. Auvergne, P. Merle, and H. Mathieu, Phys. Rev. B 12, 1371 (1975).
[32]W. Boyle and R. J. Sladek, Phys. Rev. B 11, 2933 (1975).
[33]G. L. Bir and G. E. Pikus, *Symmetry and strain-induced effects in semiconductors* (Wiley, New York, 1974), p. 419.
[34]P. Merle, D. Auvergne, and H. Mathieu, Phys. Rev. B 15, 2032 (1977), and references therein.
[35]D. L. Comphausen, G. A. Neuville Connell, and W. Paul, Phys. Rev. Lett. 26, 184 (1971).
[36]J. Balslev, J. Phys. Soc. Jpn. Suppl. 21, 101 (1966).